Separation and correlation of structural and magnetic roughness in a Ni thin film by polarized off-specular neutron reflectometry

2009 J. Phys.: Condens. Matter 21 055010

(http://iopscience.iop.org/0953-8984/21/5/055010)

J. Phys.: Condens. Matter **21** (2009) 055010 (6pp) doi:10.1088/0953-8984/21/5/055010

Separation and correlation of structural and magnetic roughness in a Ni thin film by polarized off-specular neutron reflectometry

Surendra Singh and Saibal Basu

Solid State Physics Division, Bhabha Atomic Research Centre, Mumbai-85, India

Received 10 July 2008, in final form 20 October 2008
Published 12 January 2009
Online at stacks.iop.org/JPhysCM/21/055010

Abstract

Diffuse (off-specular) neutron and x-ray reflectometry has been used extensively for the determination of interface morphology in solids and liquids. For neutrons, a novel possibility is off-specular reflectometry with polarized neutrons to determine the morphology of a magnetic interface. There have been few such attempts due to the lower brilliance of neutron sources, though magnetic interaction of neutrons with atomic magnetic moments is much easier to comprehend and easily tractable theoretically. We have obtained a simple and physically meaningful expression, under the Born approximation, for analyzing polarized diffuse (off-specular) neutron reflectivity (PDNR) data. For the first time PDNR data from a Ni film have been analyzed and separate chemical and magnetic morphologies have been quantified. Also specular polarized neutron reflectivity measurements have been carried out to measure the magnetic moment density profile of the Ni film. The fit to PDNR data results in a longer correlation length for in-plane magnetic roughness than for chemical (structural) roughness. The magnetic interface is smoother than the chemical interface.

(Some figures in this article are in colour only in the electronic version)

1. Introduction

Interfaces play a very important role in many of the interesting phenomena exhibited by magnetic films, such as magnetization reversal, magnetic anisotropy and exchange coupling of magnetic film through a non-magnetic spacer [1–3]. In giant magneto-resistance (GMR) materials interface roughness influences electron transport across interfaces [4–7]. The unidirectional anisotropy in ferromagnetic–antiferromagnetic interfaces has been successfully explained by the presence of interfacial roughness [8] which depends on magnetic roughness. There have been attempts to separate chemical and magnetic roughness and in-plane morphology using diffuse magnetic scattering of x-rays [9–13]. Specular neutron reflectivity measurements in unpolarized as well as in polarized modes have been effectively utilized to characterize the chemical and magnetic properties of thin films and multilayers [14–17]. Off-specular reflectivity measurement yields the details of lateral structure or morphology of interfaces in thin films and multilayers. Sinha *et al* [18] treated off-specular reflectivity under the Born approximation (BA) and also obtained expressions for off-specular x-ray (neutron) reflectivity under the distorted-wave Born approximation (DWBA) formalism, which was extended to stratified layer structures by Holỳ and Baumbach [19].

In the present paper we attempt complete magnetic characterization of a Ni film through specular neutron reflectometry and separation of chemical and magnetic roughness through off-specular polarized neutron reflectometry. The magnetic moment density profile of the film has been determined by specular polarized neutron reflectometry (PNR) measurements. By observing the difference in the specular polarized neutron reflectivity for the two spins of neutron parallel and antiparallel to the magnetization of a magnetic layer one can derive the magnetization profile of a ferromagnetic thin film. We have attempted to separate quantitatively the magnetic and structural roughness of the film using polarized diffuse (off-specular) neutron reflectivity (PDNR) measurements under the Born approximation [18].

The main issue addressed in this paper is the possibility of separating magnetic and chemical roughness through polarized diffuse neutron reflectivity (PDNR). We have briefly outlined the theory of polarized diffuse neutron reflectometry under the Born approximation and how the magnetic roughness can be measured. We determined magnetic moment density profile for the sample by specular polarized neutron reflectometry before performing the PDNR experiment. The magnetic moment density profile indicated that there is a reduction of magnetic moment near the surface of the sample.

2. Born approximation model of PDNR

Under the Born approximation, chemical roughness can be obtained from the height–height correlation function at the interface. The height–height correlation function itself can be obtained from Fourier transform of off-specular neutron and x-ray reflectivity data [18]. Osgood *et al* in their work on off-specular x-ray reflectivity [11] had extended the treatment for the presence of magnetic roughness along with chemical roughness by using photons of two helicities with respect to sample magnetization, also under the Born approximation. We have derived the expression for off-specular reflectivity under the Born approximation for neutrons of two polarizations with respect to in-plane sample magnetization. The scattering potential for a neutron in a magnetized medium is given by

$$V = \frac{2\pi\hbar^2}{m_n}\rho b \pm \mu B = N(b_n \pm b_m) \tag{1}$$

where μ, b_n, b_m, B and ρ are the neutron magnetic moment, nuclear scattering length, magnetic scattering length, magnetic field inside the sample and the nuclear density respectively. The $\pm$ in the potential refers to the spin up and spin down states of the incident neutrons with respect to the sample polarization.

Langridge *et al* [20] has explained the magnetic roughness by considering the orientation of magnetic domains, in the field dependence of diffuse neutron scattering on a Co/Cu multilayer system. Considering the spatially inhomogeneous magnetization profile (normal to the interface) as a random variable $\varphi(r)$, similar to local height variation in the non-magnetic case, they defined the magnetic roughness as $\sigma = \langle\varphi^2\rangle$ with correlation function $C(r) = \langle\varphi(r)\varphi(0)\rangle$. The specular polarized neutron reflectivity data show that the applied magnetic field is sufficient to saturate the in-plane magnetization of the sample and all the magnetic domains are aligned along the plane therefore we have used the following theoretical approach to analyze the PDNR data. Here we assume the existence of a structural (chemical) and a separate magnetic boundary buried below it at each interface similar to the work in [11] and [21] and we have derived a general expression for roughness for the chemical boundary and the magnetic boundary with a correlation term between the chemical and magnetic roughness similar to Osgood *et al* [11]. Figure 1(A) represents the actual boundaries, which can be then considered as really composed of two boundaries, a chemical boundary and a magnetic boundary, each with their own average height, roughness, and correlation length. The

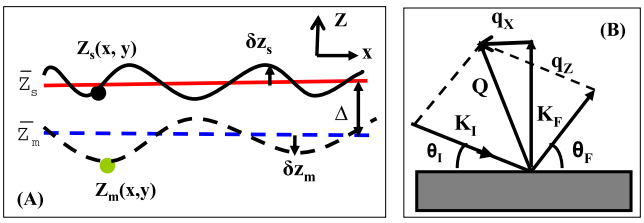

Figure 1. (A) A diagram of the structural (chemical) and magnetic boundaries at an interface. This model has been used to calculate the off-specular (diffuse) neutron reflectivity intensity from a rough interface. (B) The schematic shows the wavevectors of the incident and scattered neutron are K_I and K_F, with the incidence and exit angle θ_I and θ_F, respectively. The momentum transfer is defined by $Q = K_F - K_I = (q_x, 0, q_z)^T$.

amplitude for grazing angle neutron scattering, under the Born approximation using the potential in equation (1), is given by

$$A = \frac{Nb_n}{q_z}\int\int \mathrm{d}x\,\mathrm{d}y e^{-iq_z Z_s(x,y)} e^{-i[q_x x + q_y y]} \pm \frac{Nb_m}{q_z}\int\int \mathrm{d}x\,\mathrm{d}y e^{-iq_z Z_m(x,y)} e^{-i[q_x x + q_y y]} \tag{2}$$

where $Z_s(x, y)$ and $Z_m(x, y)$ are the heights of the structural and magnetic surfaces, respectively (see figure 1(A)). The differential cross section for scattering of neutron by this system is

$$\begin{aligned}\frac{\mathrm{d}\sigma}{\mathrm{d}\Omega} = AA^* = \frac{N^2}{q_z^2}\int\int \mathrm{d}x\,\mathrm{d}y \int\int \mathrm{d}x'\,\mathrm{d}y' \\ \times \exp\{-i[q_x(x-x') + q_y(y-y')]\} \\ \times [b_n^2 \exp\{-iq_z[Z_s(x,y) - Z_s(x',y')]\} \\ + b_m^2 \exp\{-iq_z[Z_m(x,y) - Z_m(x',y')]\} \\ \pm b_n b_m \exp\{-iq_z[Z_s(x,y) - Z_m(x',y')]\} \\ \pm b_n b_m \exp\{-iq_z[Z_m(x,y) - Z_s(x',y')]\}].\end{aligned} \tag{3}$$

In the above equation $\pm$ represents neutrons with polarization up (+) or down (−) with respect to the sample magnetization. The first two terms in the equation (3) are purely structural and purely magnetic, whereas the last two terms contain the information about magnetic as well as structural correlation. The model presented for two boundaries is valid for the case when the magnetization is collinear with the neutron polarization and applied field. We applied a permanent magnetic field for measuring PDNR data for the sample for two spins, which is sufficient for aligning the magnetic field in the plane of the film as shown by the specular polarized neutron reflectivity measurements. Using statistical averaging techniques with roughness fluctuations treated as a Gaussian random variable [18], it can be shown that the *diffuse* scattering cross section

$$\left(\frac{\mathrm{d}\sigma}{\mathrm{d}\Omega}\right)_{\mathrm{diff}} = \frac{N^2 L_x L_y}{q_z^2}[b_n^2 S_{ss} + b_m^2 S_{mm} \pm 2b_n b_m S_{sm}] \tag{4}$$

where L_x, L_y are the lateral dimension of the sample (film) and

the terms S_{nn}, etc are defined as follows:

$$S_{ss} = e^{-q_z^2\sigma_s^2} \int\int dX\, dY (e^{q_z^2 C_{ss}(X,Y)} - 1) e^{-i(q_x X + q_y Y)},$$
$$S_{mm} = e^{-q_z^2\sigma_m^2} \int\int dX\, dY (e^{q_z^2 C_{mm}(X,Y)} - 1) e^{-i(q_x X + q_y Y)},$$
$$S_{sm} = e^{-q_z^2\sigma_{sm}^2} e^{-iq_z(\bar{z}_s - \bar{z}_m)} \times \int\int dX\, dY (e^{q_z^2 C_{sm}(X,Y)} - 1) e^{-i(q_x X + q_y Y)} \quad (5)$$

where $\bar{z}_s$ and $\bar{z}_m$ are the average height of chemical (structural) and magnetic boundaries with a height deviation of δz_s and δz_m, respectively (see figure 1(A)), and the vector (X, Y) is defined as $(x - x', y - y')$. σ_s and σ_m are the root mean square values of structural and magnetic roughnesses, respectively, at the boundaries. σ_{sm} is a combination of these two roughnesses and it has been defined below. C_{ss}, C_{mm}, and C_{sm} are structural (SS), magnetic (MM), and structural–magnetic (SM) correlation functions, respectively, and defined as $C_{ss}(X, Y) = \langle \delta z_s(0) \delta z_s(R) \rangle$, $C_{mm}(X, Y) = \langle \delta z_m(0) \delta z_m(R) \rangle$, and $C_{sm}(X, Y) = \langle \delta z_s(0) \delta z_m(R) \rangle$. Here, we have assumed that both the boundaries, structural as well as magnetic, can be represented by self-affine fractal surfaces and the correlation functions can be represented as $C_{ss}(X, Y) = \sigma_s^2 \exp\{-(R/\xi_s)^{2h_s}\}$, $C_{mm}(X, Y) = \sigma_m^2 \exp\{-(R/\xi_m)^{2h_m}\}$. Here ξ_s and ξ_m are the in-plane height–height correlation lengths at the structural and magnetic boundaries, respectively. The Hurst parameter, h, is the roughness exponent describing how jagged the interface is. The Hurst parameter is restricted to the region $0 < h < 1$ and defines the fractal box dimension $D = 3 - h$ of the interface. It can be shown easily that $\sigma_{sm}^2 = (\sigma_s^2 + \sigma_m^2)/2$. We further have assumed that $\xi_{sm} = \sqrt{(\xi_s^2 + \xi_m^2)/2}$ and $h_{sm} = (h_s + h_m)/2$ define the structural–magnetic correlation function C_{sm}. It is important to note that if the structural and magnetic surfaces are completely uncorrelated (i.e. $C_{sm}(X, Y) = 0$) then S_{sm} vanishes, and only the first two terms in equation (4) will contribute to the diffuse scattering. In this case the diffuse scattering intensity for spin up and spin down neutrons remains the same. We found from the PDNR data that there was large difference between the off-specular intensities of up and down polarized neutrons, indicating that such a correlation exists in the present sample.

3. Sample and experimental set-up

The sample we studied in this work is a Ni film of ∼1500 Å, deposited on a float glass plate by a thermal evaporation method; a detailed structural characterization of the sample is given elsewhere [22]. The specular and off-specular neutron reflectometry data from the sample have been collected with a polarized neutron reflectometer, at the Dhruva reactor, Mumbai [23], designed for vertical sample geometry and using a neutron beam of variable horizontal divergence. In this instrument we used a $_2He^3$ gas-based linear position sensitive detector (PSD), placed normal to the beam path, which helps immensely to collect the data for off-specular reflectivity along with specular data without any detector movement. Figure 1(B) shows the wavevectors of the incident and scattered neutron to be K_I and K_F, with the incidence and exit angle θ_I and θ_F, respectively. The momentum transfer, $Q = K_F - K_I = (q_x, 0, q_z)^T$ is given by $q_x = K_I(\cos\theta_I - \cos\theta_F)$ and $q_z = K_I(\sin\theta_I + \sin\theta_F)$. Therefore a specular reflectivity scan ($\theta_I = \theta_F$) corresponds to a q_z scan with $q_x = 0$. The diffuse scattering data were collected along the length of the position sensitive detector (X-direction), integrated over the vertical direction (Y-direction), centered on a specular peak. This is equivalent to a detector scan in a conventional θ–2θ spectrometer for x-ray reflectivity [24]. For collecting data in a polarized mode we applied a magnetic field of 2 kG to saturate the in-plane magnetization of the sample at room temperature.

4. Results and discussion

4.1. Specular reflectivity measurements

We performed the specular reflectivity measurement on the sample using both polarized as well as unpolarized neutrons. A detailed analysis of unpolarized neutron reflectivity measurements, which gave details of the layered structure (e.g. density, thickness and roughness) of the film, was reported earlier [22]. The study showed that there are two Ni layers with different densities on top of the substrate. The thickness (density) of the top and bottom Ni layers is 235 Å (50% of bulk Ni) and 1200 Å (90% of bulk Ni), respectively. The reduction in density of the top 235 Å Ni layer was attributed to atmospheric corrosion of the film for over 15 years. Therefore unpolarized neutron reflectometry study of the Ni film has predicated a layered structure with three interfaces as shown in the inset of figure 2(A): (a) uppermost air–film interface, (b) high density layer/low density layer interface and (c) substrate/high density layer interface.

The PNR data are presented in figure 2(A). Closed and open circles are the measured reflectivity for spin up (R^+) and spin down (R^-) neutrons. Continuous lines show the best fit for corresponding neutron spins. Figure 2(B) shows the plot of spin asymmetry (ASYM), which is defined as ASYM $= (R^+ - R^-)/(R^+ + R^-)$, where $R^{+(-)}$ is the spin up (down) reflectivity. The ASYM allows a direct comparison of the difference in the neutron reflectivity due to the spin dependent magnetic interaction. The oscillations in the ASYM spectra are related to the layer thickness while the amplitude is related to the magnitude of the magnetic moment and, to a much smaller extent, to the interface roughness. For analyzing polarized specular data we have only varied the magnetic moment of the Ni film; other parameters (thickness and density), obtained from unpolarized neutron reflectivity, were kept fixed. We have used the spin-asymmetry form of data to estimate the magnetic moment, which has the advantage that it is sensitive to the magnetic moment (the sole cause of asymmetry) and less sensitive to interface roughness. We found a average roughness of ∼9 Å for all interfaces. Closed circles and the solid line in figure 2(B) represent the ASYM experimental data and the best fit to ASYM data, respectively. The best fit to PNR data and ASYM function gives the average magnetic moment per Ni atom in each Ni layer. The average magnetic moments of Ni

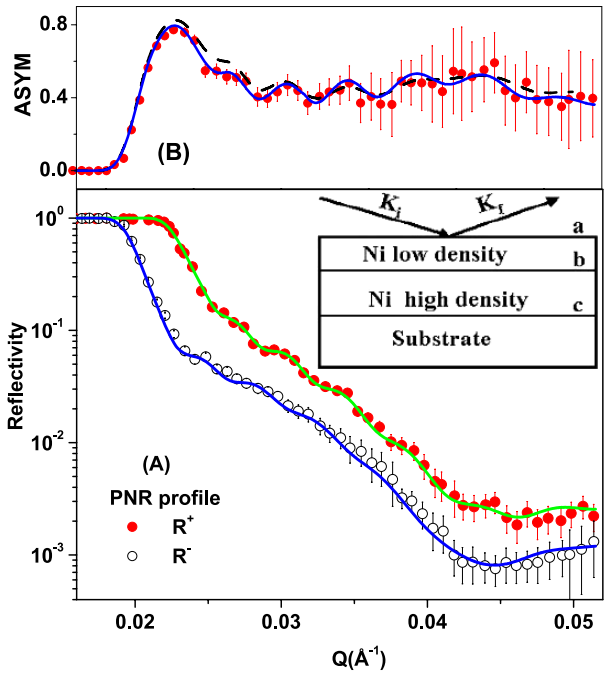

Figure 2. (A) Specular polarized neutron reflectometry data from the sample. Closed circles and open circles are the experimental data for spin up (R^+) and spin down (R^-) neutron as a function of q_z. Continuous lines are the best fit. The inset of (A) shows the layer model of the sample extracted from the best fit to previous specular unpolarized [20] neutron reflectivity measurements. (B) The spin asymmetry (ASYM), defined in the text, is plotted against q_z. Closed circles are the experimental data for (R^+) and (R^-) neutrons. The solid line shows the fit to ASYM data.

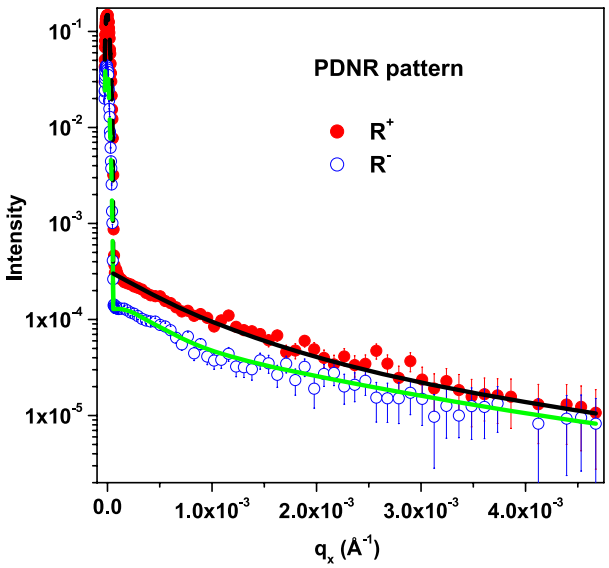

Figure 3. Off-specular polarized neutron reflectivity measurements from the sample. Closed and open circles are the experimental data for spin up and spin down neutrons, respectively, at $q_z = 0.0252$ Å^{-1}. Continuous lines are the best fit.

atoms, for the top (low density) and bottom (high density) Ni layers, obtained from the best fit to measured data are 0.33 μ_B and 0.55 μ_B, respectively, which are smaller than the bulk moment of 0.60 μ_B per Ni atom. The magnetic moment of a Ni atom in top layer is about 50% of the bulk moment. The dashed line in the spin-asymmetry plot in figure 2(B) represents a fit to the data assuming zero magnetic moment of Ni in the top, low density Ni layer of thickness 235 Å, which also authenticates the nonexistence of an oxide layer of the entire thickness of 235 Å. A previous study [22] suggested that the reduction in density of the top 235 Å Ni layer was a result of propagation of void networks in the Ni film over a period of time and not due to any chemical change. Therefore, in present case the Ni atoms in the top layers reside in a different environment with reduced nearest neighbors, which might be the major factor contributing to a reduction in the magnetic moment of Ni atoms in this layer. Chakraborty *et al* [25], in their first-principles calculation on surface magnetism of Ni atoms, have shown the effect of coordination number on the magnetic moment of a Ni atom at the surface layer. They found a reduction in the magnetic moment of a Ni atom from 0.56 to 0.25 μ_B on reducing the coordination number of the nearest neighbor from 1 to 4.

4.2. Off-specular reflectivity measurements

Figure 3 depicts the PDNR data for spin up (R^+) and spin down (R^-) neutrons measured at $q_z = 0.0252$ Å^{-1}. Closed and open circles are the experimental data for spin up and spin down neutrons, respectively. We have collected the data centered on a specular peak beyond the total reflection region but remaining in the weak scattering region where the Born approximation is valid. The diffuse data have been analyzed under the Born approximation given in section 2. For the off-specular data we positioned the specular peak at one end of the detector, to reach the largest possible value of the in-plane momentum transfer (q_x), to test the quality of fit over a large q_x range. Over the entire q_x range there is large difference in intensity between the up and down polarized beams. This is due to the S_{sm} term in equation (5), signifying the existence of correlation between structural and magnetic boundary. In the absence of such a correlation both the spin up and down intensities should be the same. Continuous lines in figure 3 are fits to the data using the model described in section 2. The dashed lines for R^+ and R^- at the specular peak position are guides to the eye only for the resolution broadened peaks. The structural morphology of the interface was determined earlier by unpolarized off-specular reflectivity [22] under the DWBA approximation using a program by Holý *et al* [19]. Parameters for chemical boundaries were reported in [22]. In the present work we have obtained the morphological parameters for the chemical and the magnetic boundaries together for the exposed surface of the film under the Born approximation from the fit of equation (4) to our data. The parameters for chemical (structure) surfaces, i.e. σ_s, ξ_s, and h_s, obtained from the best fit to the unpolarized diffuse scattering data were kept fixed while analyzing the off-specular reflectivity in polarized mode. The values of σ, ξ, and h obtained from the best fit to PDNR data are given in table 1 with subscripts 's' for the chemical boundary and 'm' for the magnetic boundary. The best fit to the diffuse data gave an average rms roughness, $\sigma_m = 4.0$ Å for the magnetic surface of interface (a). This value is marginally

Table 1. Results of the polarized off-specular neutron reflectivity measurements. Typical errors on the parameters are $\leqslant 5\%$.

	Roughness (Å)		Correlation length (Å)		Hurst parameter	
	σ_s	σ_m	ξ_s	ξ_m	h_s	h_m
Interface (a)	6.5	4.0	820	1255	0.52	0.83
Interface (b)	9.6	9.0	385	400	0.87	0.90
Interface (c)	10	10	2000	2000	0.49	0.54

lower than the structural roughness of 6.5 Å for the chemical boundary. The large differences in the correlation lengths and Hurst parameters between the chemical boundary and the magnetic boundary as obtained from the fits are the most significant results in this experiment. The correlation length for the magnetic boundary is 1255 Å which is large compared to the corresponding correlation length 820 Å for the chemical boundary. The Hurst parameters 'h' for the magnetic and chemical boundaries are 0.83 and 0.52, respectively. These parameters signify that the magnetic boundary is less 'jagged' than the chemical boundary and the height of the magnetic boundary remains correlated over a longer distance. The PDNR data also gave similar correlation parameters for the magnetic boundary (σ_m, ξ_m and h_m) and the chemical boundary (σ_s, ξ_s and h_s) for interface (b). Since interface (b) indicates a transition from a high density to low density Ni layer in our model it is not expected to have any true transition or magnetically dead layer. The result of the fit is merely a confirmation of this physical fact. This is in line with earlier studies by diffuse x-ray resonant magnetic scattering [9] and diffuse x-ray scattering [26] for magnetic interfaces. Cable *et al* [27] had conjectured earlier, using polarized neutron measurements, that the magnetic interface can be smoother than the chemical interface in Ni–Mo metallic superlattices. While such a result is understandable intuitively, we must emphasize that the exact values of these parameters for the chemical and magnetic boundaries have been obtained through the fitting of the model embedded in equation (4). It is apparent from table 1 that the magnetic boundary for interface (a) is much smoother ($h_m = 0.83$) than the chemical boundary ($h_s = 0.52$). The chemical boundary for interface (a) shows a highly fractal nature with fractal dimension $D = 2.48$, whereas the magnetic boundary is an almost two-dimensional Gaussian surface. We have carried out a detailed error analysis on the parameters obtained in our fit by the technique outlined in [28]. Typical errors on the estimated parameters are $\leqslant 5\%$.

Two issues need to be resolved before we accept the results of the fit regarding the interface morphology in the film. These are: (i) what will be the best fit if the magnetic and chemical boundaries of interface (a) are uncorrelated; and (ii) is it possible to fit a single set of parameters σ, ξ and h for both the boundaries (chemical and magnetic)? In figure 4 we have plotted the experimental data for R^+ (closed triangles) and R^- (open triangles) neutrons along with the fits for the above two cases: (i) uncorrelated chemical and magnetic boundaries, i.e. $C_{sm}(X, Y) = 0$ in equation (5). In this case the fit (star with line) does not match the experimental

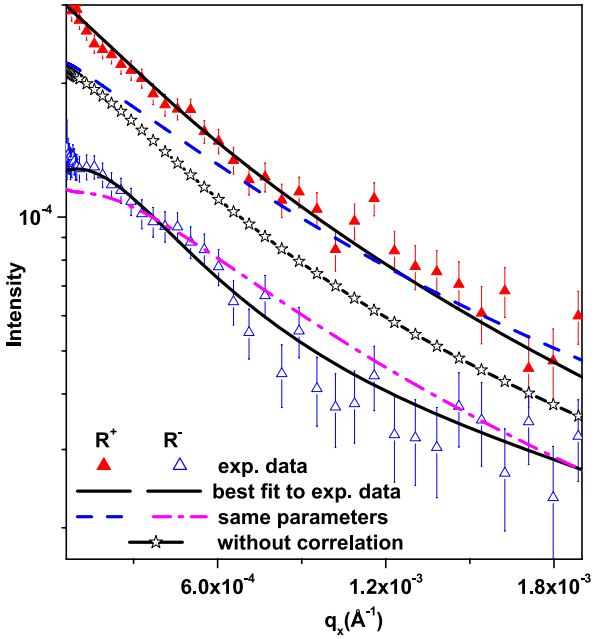

Figure 4. A comparison of morphological parameters for two boundaries (i.e. chemical and magnetic) of interface (a). Closed and opened triangles are the experimental data for R^+ and R^-. The star with the line is the fit for $C_{sm}(X, Y) = 0$ in equation (5). Dash–dash and dash–dot–dash lines are fits for same morphological parameters for $C_{ss}(X, Y)$ and $C_{mm}(X, Y)$ in equation (5). Continuous lines are best fits assuming different morphological parameters (e.g. σ, ξ, and h) for chemical and magnetic boundaries of interface (a).

data. (ii) For the same set of morphological parameters (e.g. σ, ξ and h) for chemical and magnetic boundaries the fits obtained are shown by dash–dot–dash (R^+) and dash–dash (R^-) lines. In comparison with the above cases, it is clearly seen that the best fits obtained for the model with two boundaries (chemical and magnetic) with different sets of morphological parameters shown by the continuous lines in this figure for R^+ and R^- are more appropriate for the experimental data.

To render the morphologies of two boundaries (chemical and magnetic) of interfaces (a) we have used a midterm displacement method for generating fractal surfaces [22, 29]. For this rendition of the interfaces, we have used the morphological parameters (σ, ξ and h) of two boundaries extracted from PDNR measurements (table 1). Figure 5 shows a two-dimensional plot of the chemical (curve S) and magnetic (curve M) boundaries of interface (a). The chemical boundary (curve S) has sharp undulations that are not present in the magnetic boundary. The square grids represent squares with sides of length 2ξ for both the plots. Comparison of two boundaries (S) and (M) clearly demonstrates that the magnetic boundary for interface (a) is much smoother ($h_m = 0.83$) then the chemical boundary ($h_s = 0.52$). The chemical boundary for interface (a) shows a highly fractal nature with fractal dimension $D = 2.48$, whereas the magnetic boundary is smoother and nearly two-dimensional. Also the correlation length of the magnetic boundary is higher than that for the chemical boundary.

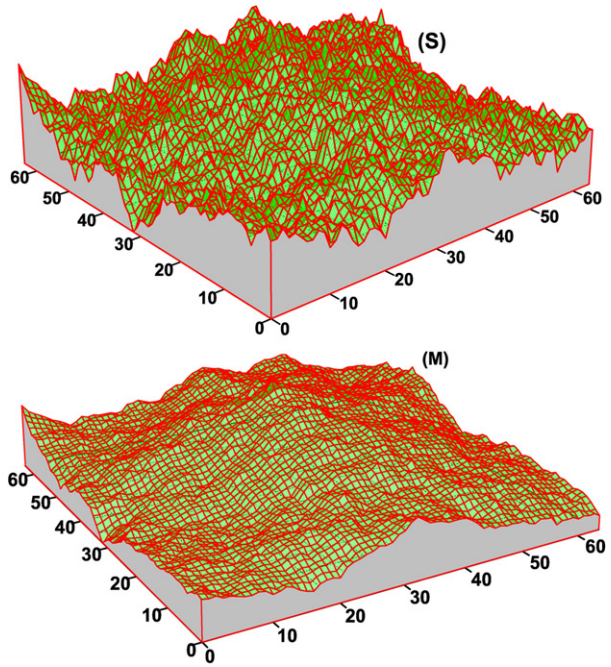

Figure 5. Two-dimensional surfaces for chemical (S) and magnetic (M) boundaries of interface (a) generated using the midpoint displacement method for fractal surfaces (see the text).

5. Summary and conclusion

In summary we have measured the magnetic moment density profile of a Ni film using polarized neutron reflectivity. We found a reduction in magnetic moment of the Ni atom on the top 235 Å thick low density Ni layer, which might have resulted mainly due to structural change cause by atmospheric corrosion. We have shown that polarized diffuse neutron reflectometry from the surface of a magnetized thin film can reveal the morphology of the magnetic interface buried below the chemical interface. The data in this case have been treated under the Born approximation, which provides a simple and physically meaningful comprehensive expression revealing various types of correlations present between these two interfaces. The parameters of lateral structure (rms roughness, correlation length, and the Hurst parameter) of interfaces for the chemical and magnetic boundaries are separated quantitatively. By extracting this information from diffuse neutron reflectometry fits we have demonstrated that the magnetic boundary shows a higher in-plane correlation length with a smoother interface. In this exploratory experiment and data treatment we have strived to demonstrate that diffuse polarized neutron reflectometry can be used as a powerful tool to look at magnetic and chemical interfaces simultaneously.

References

[1] Suzuki M and Taga Y 1995 *Phys. Rev.* B **52** 361
[2] Yang Z J and Scheinfein M R 1995 *Phys. Rev.* B **52** 4263
[3] Parkin S S P, Farrow R F C, Marks R F, Cebollada A, Harp G R and Savoy R J 1994 *Phys. Rev. Lett.* **72** 3716
[4] Grunberg P, Schreiber R, Pang Y, Brodsky M B and Sowers H 1986 *Phys. Rev. Lett.* **57** 2442
[5] Levy P M, Zhang S and Fert A 1990 *Phys. Rev. Lett.* **65** 1643
[6] Fullerton E E, Kelly D M, Guimpel J, Schuller I K and Bruynseraede Y 1992 *Phys. Rev. Lett.* **68** 859
[7] Speriosu V S, Nozieres J P, Gurney B A, Dieny B, Huang T C and Lefakis H 1993 *Phys. Rev.* B **47** 11579
[8] Takano K, Kodama R H, Berkowitz A E, Cao W and Thomas G 1997 *Phys. Rev. Lett.* **79** 1130
[9] McKay J F, Teichert C, Savage D E and Lagally M G 1996 *Phys. Rev. Lett.* **77** 3925
[10] Freeland J W, Chakarian V, Bussmann K, Idzerda Y U, Wende H and Kao C-C 1998 *J. Appl. Phys.* **83** 6290
[11] Osgood R M III, Sinha S K, Freeland J W, Idzerda Y U and Bader S D 1999 *J. Magn. Magn. Mater.* **198** 698
[12] Idzerda Y U, Chakarian V and Freeland J W 1999 *Phys. Rev. Lett.* **82** 1562
[13] Fischer P, Eimuller T, Schutz G, Guttmann P, Schmahl G, Pruegl K and Bayreuther G 1998 *J. Phys. D: Appl. Phys.* **31** 649
[14] Blundell S J and Bland J A C 1992 *Phys. Rev.* B **46** 3391
[15] Bland J A C (ed) 1994 *Polarised Neutron Reflection* (*Ultrathin Magnetic Structures* vol I) (Berlin: Springer) pp 305–42
[16] Felcher G P, Gray K E, Kampwirth R T and Brodsky M B 1986 *Physica* B **136** 59
[17] Majkrzak C F, Cable J W, Kwo J, Hong M, Mcwhan D B, Yafet Y and Waszcak J 1986 *Phys. Rev. Lett.* **56** 2700
[18] Sinha S K, Sirota E B, Garoff S and Stanley H B 1988 *Phys. Rev.* B **38** 2297
[19] Holý V and Baumbach T 1994 *Phys. Rev.* B **49** 10668
[20] Langridge S, Schmalian J, Marrows C H, Dekadjevi D T and Hickey B J 2000 *Phys. Rev. Lett.* **85** 4964
[21] Lee D R, Sinha S K, Haskel D, Choi Y, Lang J C, Stepanov S A and Srajer G 2003 *Phys. Rev.* B **68** 224409
[22] Singh S and Basu S 2006 *Surf. Sci.* **600** 493
[23] Basu S and Singh S 2006 *J. Neutron Res.* **14** 109
[24] Schlomka J P, Tolan M, Schwalowsky L, Seeck O H, Stettner J and Press W 1995 *Phys. Rev.* B **51** 2311
[25] Chakraborty M, Mookerjee A and Bhattacharya A K 2005 *J. Magn. Magn. Mater.* **285** 210
[26] Kelly J J IV, Barnes B M, Flack F, Lagally D P, Savage D E, Friesen M and Lagally M G 2002 *J. Appl. Phys.* **91** 9978
[27] Cable J W, Khan M R, Felcher G P and Schuller I K 1986 *Phys. Rev.* B **34** 1643
[28] Press W H, Teukolsky S A, Vetterling W T and Flannery B P 2005 *Numerical Recipes in FORTRAN, The Art of Scientific Computing* 2nd edn (Cambridge: Cambridge University Press)
[29] Peitgen H-O and Saupe D (ed) 1988 *The Science of Fractal Images* (New York: Springer)